Published by Institute of Physics Publishing for SISSA/ISAS
Received: *November 19, 2003*
Revised: *July 6, 2004*
Accepted: *August 2, 2004*

Dynamical overlap fermions, results with hybrid Monte-Carlo algorithm

Zoltan Fodor,[ab] **Sandor D. Katz**[ac*] **and Kalman K. Szabó**[ab]

[a] *Department of Physics, University of Wuppertal Germany*
[b] *Institute for Theoretical Physics, Eötvös University Budapest, Hungary*
[c] *Deutsches Elektronen-Synchrotron DESY Hamburg, Germany*
E-mail: fodor@bodri.elte.hu, sandor.katz@desy.de, szaboka@general.elte.hu

Abstract: We present first, exploratory results of a hybrid Monte-Carlo algorithm for dynamical, $n_f = 2$, four-dimensional QCD with overlap fermions. As expected, the computational requirements are typically two orders of magnitude larger for the dynamical overlap formalism than for the more conventional (Wilson or staggered) formulations.

Keywords: Lattice Gauge Field Theories, Lattice QCD.

JHEP08(2004)003

[*] On leave from Institute for Theoretical Physics, Eötvös University, Budapest, Hungary.

Contents

1. Introduction

Fermionic operators (D) satisfying the Ginsparg-Wilson relation [1]

$$\gamma_5 D + D\gamma_5 = \frac{1}{m_0} D\gamma_5 D \tag{1.1}$$

allow to solve the chirality problem of four-dimensional QCD at non-vanishing lattice spacing [2]–[9](for different reviews at recent lattice conferences see e.g. [10]–[18]).

Clearly, it would be very useful to exploit these new developments in numerical studies of QCD. In the past years several groups have calculated already e.g. the quenched hadron spectrum and light quark masses with better and better accuracies (for recent results see the overlap formulation [19]–[22] and a related work with the perfect and chirally improved actions [23]).

Due to limitations in computational resources no result is available for dynamical, four-dimensional QCD with Ginsparg-Wilson fermions. Some exploratory studies were carried out in the Schwinger model and suggestions were made, which could help the four-dimensional full QCD case [24]–[31]. Note, however, that first results are already available for dynamical domain-wall fermions [32]. It would be of extreme importance to compare the necessary computational costs of the domain-wall and the overlap formulations. Unfortunately today very little is known about the mass and volume dependence of the existing — and hopefully improving — algorithms. In order to reach a quantitative comparison, large scale simulations are needed.

In this letter we present exploratory tests using dynamical, four-dimensional QCD with Ginsparg-Wilson fermions. We start with the Zolotarev optimal rational polynomial approximation [33]. The partial fraction expansion of the rational polynoms leads to a particularly simple expression for the fermionic force of the hybrid Monte-Carlo. In addition to the usual fermion matrix inversion we have another inversion due to the inverse in the partional fraction expansion. These nested inversions are very CPU consuming. By projecting out the smallest eigenmodes in the inner loop a significant speed up could be reached.

As we emphasized, our results are exploratory. In addition they are obtained on absurdly small lattices. As usual, direct physical interpretation will be possible only after studying larger lattices and approaching the continuum limit. Nevertheless, these first results can be used as references in order to cross check future studies.

2. Hybrid Monte-Carlo for QCD with overlap fermions

First we fix our notations. The massless Neuberger-Dirac operator (or overlap operator) D can be written as

$$D = m_0[1 + \gamma_5 \,\mathrm{sgn}(H_W)]\,, \tag{2.1}$$

This D operator satisfies eq. (1.1). H_W is the hermitian Dirac operator, $H_W = \gamma_5 D_W$, which is built from the massive Wilson-Dirac operator, D_W, defined by

$$[D_W]_{xy} = \delta_{xy} - \kappa_W \sum_\mu \left\{U_\mu(x)(1+\gamma_\mu)\delta_{x,y-\mu} + U^\dagger_\mu(y)(1-\gamma_\mu)\delta_{y,x+\mu}\right\},$$

where κ_W is related to m_0 by $\kappa_W^{-1} = 4 - m_0/2$. The mass is introduced in the overlap operator by

$$D(m) = (1-m)D + m\,. \tag{2.2}$$

In the sign function of eq. (2.1) one uses $\mathrm{sgn}(H_W) = H_W/\sqrt{H_W^2}$. The n^{th} order Zolotarev optimal rational approximation for $1/\sqrt{x}$ in some interval $[1, x_{\max}]$ can be expressed by elliptic functions (see e.g. [34]). For most of the purposes a more transparent suboptimal choice $\epsilon(x)$ with $\epsilon(1) = 1$ is sufficient[1]

$$\mathrm{sgn}(x) \approx \epsilon(x) = x \prod_{l=1}^{n} \frac{(x^2 + c_{2l})/(1+c_{2l})}{(x^2 + c_{2l-1})/(1+c_{2l-1})}, \tag{2.3}$$

where

$$c_l = \frac{\mathrm{sn}^2(lK/(2n+1);\kappa)}{1-\mathrm{sn}^2(lK/(2n+1);\kappa)}\,, \qquad \kappa = \sqrt{1 - \frac{1}{x_{\max}}}\,, \tag{2.4}$$

the jacobian elliptic function $\mathrm{sn}(u,\kappa) = \eta$ is defined by the elliptic integral

$$u(\eta) = \int_0^\eta \frac{dt}{\sqrt{(1-t^2)(1-\kappa^2 t^2)}}\,, \tag{2.5}$$

and $K = u(1)$ is the complete elliptic integral. A particularly useful form of eq. (2.3) and an approximation for the sign function is given by partional fractioning

$$\epsilon(x) = x(x^2 + c_{2n}) \sum_{l=1}^{n} \frac{b_l}{x^2 + c_{2l-1}}\,, \tag{2.6}$$

where the b_l parameters are expressed by the c_l coefficients of eq. (2.4). In the rest of the paper we use the approximate $\epsilon(x)$ instead of the sign function in the Dirac operator

$$D = m_0[1 + \gamma_5 \epsilon(h_W)]\,, \tag{2.7}$$

[1] In our test we use a 20th order approximation with e.g. $x_{\max} = 10^{11}$. It is easy to check that this choice corresponds to a relative accuracy of $\mathcal{O}(10^{-5})$. The difference between the optimal and suboptimal choices is one order of magnitude smaller.

JHEP08(2004)003

where we normalize H_W by its smallest eigenvalue: $h_W = H_W/|\lambda_{\min}|$. This choice ensures that all the eigenvalues of h_W^2 are within the interval $[1, x_{\max}]$ where $x_{\max}$ is taken to be larger than the condition number of H_W.

We follow the standard procedure to implement the fermionic operator of eq. (2.1) into a hybrid Monte-Carlo [35] QCD algorithm. We analyze two flavours, thus $D^\dagger D$ is used as the Dirac operator. The fermionic determinant for these two flavours can be given by introducing the pseudofermionic fields

$$\det(D^\dagger D) = \int d\phi^\dagger d\phi \exp(-S_p) \qquad \text{with} \qquad S_p = \phi^\dagger (D^\dagger D)^{-1} \phi \,. \tag{2.8}$$

As usual, the integral is calculated stochastically by generating Gauss distributed ϕ pseudofermions. The contribution of the pseudofermions to the force has the usual form

$$\frac{dS_p}{dU} = -\psi^\dagger \frac{dD^\dagger D}{dU} \psi \qquad \text{with} \qquad \psi = (D^\dagger D)^{-1} \phi \,. \tag{2.9}$$

Compared to the hybrid Monte-Carlo with Wilson fermions the new feature is the somewhat more complicated structure of the overlap operator. This complication is threefold.

(a) First of all, it appears in the inversion of the fermion operator.

(b) Secondly, the complication is present in the structure of the derivative term in the fermionic force.

(c) Thirdly, the fermion force has Dirac-delta type singularities.

Ad (a). The inversion of the fermion operator $\psi = (D^\dagger D)^{-1}\phi$ is done by n_o conjugate gradient steps ("outer inversion"). Note, however, that each step in this procedure needs the calculation of $(D^\dagger D)\phi$. The operator D contains $\epsilon(h_W)$, which is given by the partional fraction expansion (see eq. (2.6)). Thus, at each "outer" conjugate gradient step one needs n different inversions. Fortunately, these inversions differ only by a constant term c_{2l-1} ($l = 1, \ldots, n$). It means, that this "inner inversion" can be done by one multi-shift conjugate gradient [27] procedure in n_i steps, and one is not forced to carry out n different conjugate gradient inversions. This nested conjugate gradient procedure needs all together $n_o \cdot n_i$ matrix-vector multiplications. It is already well known from the quenched analysis, that the number of steps in the inner inversion can be significantly reduced by projecting out the smallest eigenmodes and performing the conjugate gradient steps only in the orthogonal subspace.

Ad (b). In the fermionic force the derivative with respect to the link variable U can be straightforwardly calculated from the partial fraction expansion eq. (2.6). The term coming from the ϵ function reads

$$\begin{aligned} \psi^\dagger \gamma_5 \frac{d\epsilon(h_W)}{dU} \psi = \psi^\dagger \gamma_5 \sum_{l=1}^{n} \Bigg\{ & \frac{dh_W}{dU}(h_W^2 + c_{2n}) + \\ & + (c_{2l-1} - c_{2n}) \frac{h_W}{h_W^2 + c_{2l-1}} \left(h_W \frac{dh_W}{dU} + \frac{dh_W}{dU} h_W \right) \Bigg\} b_l \psi_l \,, \end{aligned} \tag{2.10}$$

where the definition

$$\psi_l = (h_W^2 + c_{2l-1})^{-1}\psi \tag{2.11}$$

was introduced. In order to calculate the force one has to determine ψ_l. The above inversion for the force is done by a multi-shift conjugate gradient process in additional n_f steps. Note, however, that this inversion increases the computational effort only marginally. Having obtained ψ in $(n_o \cdot n_i)$ multiplication steps, ψ_l can be obtained just by inverting $h_W^2 + c_{2l-1}$. All together the determination of ψ_l needs $(n_o \cdot n_i + n_f)$ matrix-vector multiplications.

Ad (c)**.** Since the fermionic force is the derivative of a non-analytic function, we expect non-trivial behaviour near these non-analyticities. This feature is already present in a classical one-dimensional motion of a point-particle in a step function potential. A finite stepsize integration of the equation of motion will not notice the step in the potential or the Dirac-delta in the force. As a consequence the action has a large change which might lead to bad acceptance rate in the Monte-Carlo simulations. One can improve on this situation. During the integration one should check whether the particle moved from one side to the other one of the step function. If it is necessary, one corrects its momentum and position. This correction has to be done also in the case of the overlap fermion. The microcanonical energy,

$$\mathcal{H} = \frac{1}{2}\langle H, H\rangle + S_{\text{gauge}}[U] + S_{\text{p}}[U,\phi] = \frac{1}{2}\langle H, H\rangle + S[U,\phi] \tag{2.12}$$

has a step function type non-analyticity on the the zero-eigenvalue surfaces of the H_W operator in the space of link variables coming from the pseudofermion action. In eq. (2.12) the $\langle A, B\rangle = -\sum_{x,\mu} \text{tr}(A_{x,\mu}B_{x,\mu})$ scalar product and H anti-hermitian gauge momenta were introduced. When the microcanonical trajectory reaches one of these surfaces, we expect either reflection or refraction. If the momentum component, orthogonal to the zero-eigenvalue surface, is large enough to compensate the change of the action between the two sides of the singularity (ΔS) then refraction should happen, otherwise the trajectory should reflect off the singularity surface. Other components of the momenta are unaffected. The anti-hermitian normal vector (N) of the zero-eigenvalue surface can be expressed with the help of the gauge derivative (in our shorthand notation $D\lambda$) as

$$N = \left.\frac{D\lambda}{\sqrt{\langle D\lambda, D\lambda\rangle}}\right|_{\lambda=0},$$

where $D\lambda = \langle\lambda|DH_W|\lambda\rangle$. Table 1 summarizes the conditions of refraction and reflection and the new momenta.

We have to modify the standard leap-frog integration of the equations of motion in order to take into account reflection and refraction. This can be done in the following way. The standard leap-frog consists of three steps: an update of the links with stepsize $\tau/2$, an update of the momenta with τ and finally another update of the links, using the new momenta, again with $\tau/2$, where τ is the stepsize of the integration. The system can only reach the zero-eigenvalue surface during the update of the links. We have to identify the step in which this happens. This can be done by predicting the change of the lowest

JHEP08(2004)003

	When	New momenta
Refraction	$\langle N,H\rangle^2 > 2\Delta S$	$H - N\langle N,H\rangle + N\langle N,H\rangle\sqrt{1-2\Delta S/\langle N,H\rangle^2}$
Reflection	$\langle N,H\rangle^2 < 2\Delta S$	$H - 2N\langle N,H\rangle$

Table 1: Refraction and reflection can happen to the system when approaches a zero-eigenvalue surface of H_W. The conditions and the new momenta are indicated. H is the momentum before the refraction/reflection.

eigenvalues during one elementary link update using the derivatives $D\lambda$. At the stepsizes we used, this procedure turned out to be very reliable. After identifying the step in which the zero eigenvalue surface is reached, we have to replace it with the following three steps:

1. Update the links with τ_1, so that we reach exactly the zero-eigenvalue surface. τ_1 can be determined with the help of $D\lambda$.

2. Modify the momenta according to table 1.

3. Update the links using the new momenta, with stepsize $\tau/2 - \tau_1$.

This procedure is trivially reversible and it also preserves the integration measure (see appendix).

Including reflection and refraction into the update is a crucial point in the simulations. If the system does not notice the step in the action due to the finite stepsize integration, there will be huge jumps in the energy leading to a very bad acceptance ratio in the final accept/reject step.

3. Numerical tests

As it was discussed by many authors (and we also illustrated above) the dynamical hybrid Monte-Carlo for QCD with overlap fermions is computationally extremely intensive due to the nested inversion. $\mathcal{O}(100)$ conjugate gradient steps is usually enough for Wilson or staggered fermions. In the overlap formalism one is confronted with $\mathcal{O}(100^2)$ matrix-vector multiplications. Therefore, with a straightforward hybrid Monte-Carlo and with present medium-size machines only absurdly small lattices can be studied. Nevertheless, these studies can show the feasibility of the algorithm and can be used for cross-checking future results.

We studied our hybrid Monte-Carlo on $V = 2^4, 4^4$ and on $4 \cdot 6^3$ lattices with $m_0 = 1.6$, with mass parameters $m = 0.1, 0.2$ and β between 5.3 and 6.1. The length of our trajectories were 1. We used $\Delta\tau = 0.01$–0.05 as time-steps for the molecular dynamical evolution. The Metropolis accept/reject step at the end of the trajectories resulted in a 30-80% acceptance rate.

We used a 20th order rational polynomial approximation. This choice gives the sign function with a relative accuracy of $\mathcal{O}(10^{-5})$. Note, that changing the order of the approximation from 10 to 20 increased the computational effort only by 20%.

JHEP08(2004)003

V	(β,m)	number of trajectories	Plaquette
2^4	$(5.6, 0.2)$	900	3.44(1)
4^4	$(5.4, 0.2)$	1200	2.572(4)
$4 \cdot 6^3$	$(5.78, 0.1)$	400	3.22(1)

Table 2: Expectation values of the plaquette variable for different volumes and parameters.

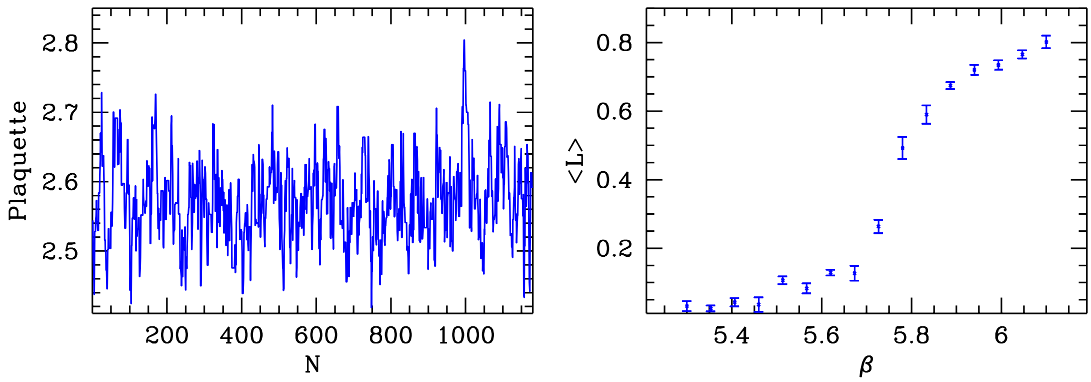

Figure 1: The time history of the plaquette (left panel) on a 4^4 lattice at $m = 0.2$ and $\beta = 5.4$. The β dependence (right panel) of the Polyakov-loop on $4 \cdot 6^3$ lattices at $m = 0.1$. (Quenched results suggest that the pion mass could be around 200–250 MeV for our parameter choice at $\beta = 5.7$).

In order to accelerate the inner inversion we projected out the eigenmodes with the smallest eigenvalues. The inversion was then performed in the orthogonal subspace. We studied the computational requirements as a function of the number of the projected eigenmodes. The projections were done by the ARPACK code. The optimum was found around 20 eigenmodes. The projection leads to an important observation. The operator H_W might have rather small eigenvalues e.g. $\mathcal{O}(10^{-6})$. In order to project out eigenmodes one has to solve eigenvalue equations. In these equations the sum of $\mathcal{O}(1)$ numbers should result in $\mathcal{O}(10^{-6})$. This is clearly beyond the accessible region of 32-bit arithmetics. Therefore, we used 64-bit precision.

In addition to the standard consistency tests (reversibility of the trajectories and $\Delta\tau^2$ scaling of the action) we performed a brute force approach on 2^2 and 4^4 lattices. We generated quenched configurations, then we explicitely calculated the determinants of $m_0[1 + \gamma_5 \epsilon(h_W)]$. These determinants were used in an additional Metropolis accept/reject step. The hybrid Monte-Carlo results agree completely with those of the brute force approach.

Table 2 gives informations on our run parameters and test results.

The left panel of figure 1 shows the time history of the plaquette variable in one of our 4^4 runs. We also observed changes between topological sectors. The ratio of topologically non-trivial and trivial gauge configurations was found to be about the same as in the brute force approach (it is around or below the percent level). On the right panel we present the β dependence of the Polyakov-loop. These runs were obtained on $4 \cdot 6^3$ lattices [36]. One can see a sharp increase around $\beta \simeq 5.7$. As usual, before drawing any physical interpretation one should proceed to the continuum limit (see also ref. [37]).

4. Conclusions

In this paper we described a hybrid Monte-Carlo algorithm for dynamical, $n_f = 2$, four-dimensional QCD with overlap fermions. We used a modified version of the MILC collaboration's code. We started with the Zolotarev optimal rational polynomial approximation to numerically implement the sign function. Using the partional fraction expansion of the rational polynomial resulted in a particularly simple form for the fermionic force. The inversions due to the fermion operator ("outer inversion") and due to the rational polynomial denominator ("inner inversion") were done successively by conjugate gradient processes. It was possible to significantly accelerate the inner inversion by projecting out the lowest eigenmodes and to use a multi-shift solver for the different terms in the partional fraction expansion.

We extended the standard leap-frog integration of the trajectories by including the refraction and reflection on the zero-eigenvalue surfaces of the Wilson-Dirac operator. The inclusion of these effects increased the acceptance rate of the algorithm significantly.

We compared our hybrid Monte-Carlo results with those obtained by a brute force approach (quenched configurations with Metropolis accept/reject steps for the exactly calculated overlap determinant). A complete agreement was found for 2^4 and 4^4 lattices.

When writing up this paper an independent hybrid Monte-Carlo was written [38]. We cross-checked the results for 4^4 lattices and a complete agreement was found.

Acknowledgments

Our tests were done by a modified version of the MILC Collaboration's public code (see `http://physics.indiana.edu/~sg/milc.html`). Numerical tests were carried out on the PC-cluster (163 Intel-P4 nodes) at the Eötvös University of Budapest, Hungary. Useful discussions and comments on the manuscript from Th. Lippert, I. Montvay, R. Narayanan and H. Neuberger are acknowledged. Special thanks go to T. Kovács for his comments and for bringing two bugs of the open ARPACK code into our attention. This work was partially supported by Hungarian Scientific grants, OTKA-T34980/T29803/T37615/-M37071/TS44839/OMFB1548/OMMU-708.

A. Area conservation of the modified leap-frog step

In this appendix we examine the area-preserving property of the modified leap-frog procedure described in the text.

Let us start with an example of the N-dimensional euclidean coordinate space which shows the basic idea of the proof in a transparent way.

We solve the equations of motion with a finite stepsize integration of the following hamiltonian:

$$\mathcal{H} = \frac{1}{2} p_a p_a + S\left(\operatorname{sgn} M(q)\right),$$

where q_a, p_a $(a = 1 \ldots N)$ are the coordinates and the momenta. M depends only on the coordinates and the action S is a smooth function (note that q_a, M and S are analogous to the links, the fermion matrix and the fermionic action, respectively). The standard leap-frog algorithm can be effectively applied to this system, as long as the trajectories do not cross the zero-eigenvalue surface of M ($\lambda(q) = 0$, where $\lambda(q)$ is the eigenvalue with smallest magnitude[2]).

We have to modify the leap-frog algorithm, when the coordinates reach the zero-eigenvalue surface. Instead of the original leap-frog update of the coordinates, where the constant p_a momenta are used for the time $\tau/2$, we first update the coordinates with p_a until the surface, then we change the momentum to p'_a, which is used to evolve q_a for the remaining time. In case of refraction one has the following phase space transformation:

$$\begin{aligned} q' &= q + \tau_1 p + \left(\frac{\tau}{2} - \tau_1\right) p' \\ p' &= p - n(np) + n(np') \end{aligned} \tag{A.1}$$

where n is the normalvector of the surface, ΔS is the potential jump along the surface, and $(np')^2 = (np)^2 - 2\Delta S$. τ_1 is the time required to reach the surface with the incoming momenta p. The transformation for reflection is given by

$$\begin{aligned} q' &= q + \tau_1 p + \left(\frac{\tau}{2} - \tau_1\right) p' \\ p' &= p - 2n(np)\,. \end{aligned} \tag{A.2}$$

In the following we will not deal with this case (one can obtain the jacobian of reflection by simply setting $(np') = -(np)$ in the jacobian of refraction).

First let us concentrate on the q, p dependence of τ_1. $\tau_1(q,p)$ is determined from the condition $\lambda(q + \tau_1(q,p)p) = 0$. One obtains the partial derivatives of τ_1 with respect to q, p by expanding this zero-eigenvalue condition to first order in δq or δp. First take the δq variation:

$$\lambda\left(q_a + \tau_1 p_a + \delta q_a + \frac{\partial \tau_1}{\partial q_b}\delta q_b p_a\right) = \lambda(q + \tau_1 p) + \left.\frac{\partial \lambda}{\partial q_a}\right|_{q+\tau_1 p}\left(\delta_{ab} + \frac{\partial \tau_1}{\partial q_b} p_a\right)\delta q_b = 0$$

Since the normalvector is just

$$n_a = \frac{\partial \lambda / \partial q_a|_{q+\tau_1 p}}{||\partial \lambda / \partial q||}\,,$$

we have for the partial derivative of τ_1 with respect to q:

$$\frac{\partial \tau_1}{\partial q_a} = -\frac{n_a}{(np)}\,.$$

Similarly one gets for the partial derivative with respect to p:

$$\frac{\partial \tau_1}{\partial p_a} = -\tau_1 \frac{n_a}{(np)}\,.$$

[2]We do not deal with the possibility of degenerate zero eigenvalues which appears only on a zero measure subset of the zero-eigenvalue surface.

JHEP08(2004)003

There is an important identity between the q and p derivatives of a function, which depends only on $q + \tau_1(q,p)p$. (Two examples are n and ΔS.) Let us evaluate p and q derivatives of an arbitrary $g(q + \tau_1(q,p)p)$ function:

$$\frac{\partial g}{\partial q_a} = \left.\frac{\partial g}{\partial q_b}\right|_{q+\tau_1 p} \left(\delta_{ab} + \frac{\partial \tau_1}{\partial q_a} p_b\right) = \left.\frac{\partial g}{\partial q_b}\right|_{q+\tau_1 p} \left(\delta_{ab} - \frac{n_a p_b}{(np)}\right),$$
$$\frac{\partial g}{\partial p_a} = \left.\frac{\partial g}{\partial q_b}\right|_{q+e_1 p} \left(\tau_1\delta_{ab} + \frac{\partial \tau_1}{\partial p_a} p_b\right) = \left.\frac{\partial g}{\partial q_b}\right|_{q+\tau_1 p} \left(\delta_{ab} - \frac{n_a p_b}{(np)}\right)\tau_1\,,$$

which gives

$$\frac{\partial g}{\partial p_a} = \tau_1 \frac{\partial g}{\partial q_a}\,. \tag{A.3}$$

Now we can consider the four different partial derivatives required for the jacobian:

$$J = \begin{pmatrix} \frac{\partial q'}{\partial q} & \frac{\partial q'}{\partial p} \\ \frac{\partial p'}{\partial q} & \frac{\partial p'}{\partial p} \end{pmatrix},$$

whose determinant gives the change in the euclidean measure $d^N q d^N p$ due to the given phase space transformation. Introducing

$$Z_{ab} \equiv \frac{\partial p'_a}{\partial q_b}\,.$$

one incorporates all terms which arise from the q dependence of the normalvector and ΔS. In case of a straight wall with constant potential jump this matrix vanishes. (Clearly, for QCD with overlap fermions these objects are very hard to calculate; they usually require the diagonalization of the whole H_W matrix). Using (A.3) the other three components of J can also be expressed with the help of Z. Denoting

$$x \equiv \frac{(np')}{(np)} - 1\,, \qquad y \equiv \frac{(np)}{(np')} - 1$$

and

$$P_{ab} \equiv \delta_{ab} + x n_a n_b\,,$$

we have

$$P^{-1}_{ab} = \delta_{ab} + y n_a n_b\,.$$

In terms of the P, P^{-1} and Z matrices the jacobian is very simple. We can split it into 2 parts: the first part is a matrix with determinant one and all Z factors are in the second term:

$$J = \begin{pmatrix} P & \tau_1 P + (\tau/2 - \tau_1)P^{-1} \\ 0 & P^{-1} \end{pmatrix} + \begin{pmatrix} (\tau/2 - \tau_1)Z & (\tau/2 - \tau_1)\tau_1 Z \\ Z & \tau_1 Z \end{pmatrix}.$$

Let us introduce J' as the product of J and the inverse of its first term:

$$J' = \begin{pmatrix} 1 & 0 \\ 0 & 1 \end{pmatrix} \otimes \mathbb{1} + E \otimes \tau_1 P Z,$$

JHEP08(2004)003

where E is defined as

$$E = \begin{pmatrix} -1 & -\tau_1 \\ 1/\tau_1 & 1 \end{pmatrix}.$$

E has an eigenvector $v_1 \propto (\tau_1, -1)$ with zero eigenvalue. The $v_2 \propto (1, \tau_1)$ vector is orthogonal to v_1 and has the property to give zero in the product $v_2^T E v_2 = 0$. In the orthonormal basis given by v_1 and v_2 J' has the form:

$$J' = \begin{pmatrix} 1 & 0 \\ 0 & 1 \end{pmatrix} \otimes \mathbb{1} + \begin{pmatrix} 0 & v_1^T E v_2 \\ 0 & 0 \end{pmatrix} \otimes \tau_1 P Z\,,$$

thus $\det J' = 1$. Since J and J' differs only in a matrix with determinant one, we arrive

$$\det J = 1\,,$$

thus the transformations (A.1), (A.2) preserve the integration measure.

The proof for the SU(3) case was carried out in a completely analogous way. The only difference was the appearance of factors associated with the group structure of SU(3) which all canceled out in the final result. Thus, we conclude that the suggested modification of the leap-frog conserves the integration measure.

References

[1] P.H. Ginsparg and K.G. Wilson, *A remnant of chiral symmetry on the lattice*, *Phys. Rev.* **D 25** (1982) 2649.

[2] H. Neuberger, *Exactly massless quarks on the lattice*, *Phys. Lett.* **B 417** (1998) 141 [hep-lat/9707022].

[3] P. Hasenfratz, *Prospects for perfect actions*, *Nucl. Phys.* **63** *(Proc. Suppl.)* (1998) 53 [hep-lat/9709110].

[4] H. Neuberger, *Vector like gauge theories with almost massless fermions on the lattice*, *Phys. Rev.* **D 57** (1998) 5417 [hep-lat/9710089].

[5] P. Hasenfratz, V. Laliena and F. Niedermayer, *The index theorem in QCD with a finite cut-off*, *Phys. Lett.* **B 427** (1998) 125 [hep-lat/9801021].

[6] H. Neuberger, *More about exactly massless quarks on the lattice*, *Phys. Lett.* **B 427** (1998) 353 [hep-lat/9801031].

[7] P. Hasenfratz, *Lattice QCD without tuning, mixing and current renormalization*, *Nucl. Phys.* **B 525** (1998) 401 [hep-lat/9802007].

[8] M. Lüscher, *Exact chiral symmetry on the lattice and the Ginsparg-Wilson relation*, *Phys. Lett.* **B 428** (1998) 342 [hep-lat/9802011].

[9] H. Neuberger, *A practical implementation of the overlap-Dirac operator*, *Phys. Rev. Lett.* **81** (1998) 4060 [hep-lat/9806025].

[10] F. Niedermayer, *Exact chiral symmetry, topological charge and related topics*, *Nucl. Phys.* **73** *(Proc. Suppl.)* (1999) 105 [hep-lat/9810026].

[11] R. Narayanan, *Spectrum of the hermitian Wilson Dirac operator*, *Nucl. Phys.* **73** *(Proc. Suppl.)* (1999) 86 [hep-lat/9810045].

[12] H. Neuberger, *Chiral fermions on the lattice*, *Nucl. Phys.* **83** *(Proc. Suppl.)* (2000) 67 [hep-lat/9909042].

[13] M. Lüscher, *Chiral gauge theories on the lattice with exact gauge invariance*, *Nucl. Phys.* **83** *(Proc. Suppl.)* (2000) 34 [hep-lat/9909150].

[14] M. Golterman, *Lattice chiral gauge theories*, *Nucl. Phys.* **94** *(Proc. Suppl.)* (2001) 189 [hep-lat/0011027].

[15] Y. Kikukawa, *Analytic progress on exact lattice chiral symmetry*, *Nucl. Phys.* **106** *(Proc. Suppl.)* (2002) 71 [hep-lat/0111035].

[16] P. Hernandez, *Ginsparg-Wilson fermions: practical aspects and applications*, *Nucl. Phys.* **106** *(Proc. Suppl.)* (2002) 80 [hep-lat/0110218].

[17] C. Gattringer, *Recent results from systematic parameterizations of Ginsparg-Wilson fermions*, *Nucl. Phys.* **119** *(Proc. Suppl.)* (2003) 122 [hep-lat/0208056].

[18] L. Giusti, *Exact chiral symmetry on the lattice: QCD applications*, *Nucl. Phys.* **119** *(Proc. Suppl.)* (2003) 149 [hep-lat/0211009].

[19] P. Hernandez, K. Jansen, L. Lellouch and H. Wittig, *Non-perturbative renormalization of the quark condensate in Ginsparg-Wilson regularizations*, *J. High Energy Phys.* **07** (2001) 018 [hep-lat/0106011].

[20] L. Giusti, C. Hoelbling and C. Rebbi, *Light quark masses with overlap fermions in quenched QCD*, *Phys. Rev.* **D 64** (2001) 114508 [hep-lat/0108007].

[21] S.J. Dong, T. Draper, I. Horvath, F.X. Lee, K.F. Liu and J.B. Zhang, *Chiral properties of pseudoscalar mesons on a quenched* 20^4 *lattice with overlap fermions*, *Phys. Rev.* **D 65** (2002) 054507 [hep-lat/0108020].

[22] T.-W. Chiu and T.-H. Hsieh, *Light quark masses, chiral condensate and quark-gluon condensate in quenched lattice QCD with exact chiral symmetry*, *Nucl. Phys.* **B 673** (2003) 217 [hep-lat/0305016].

[23] BGR collaboration, C. Gattringer et al., *Quenched spectroscopy with fixed-point and chirally improved fermions*, *Nucl. Phys.* **B 677** (2004) 3 [hep-lat/0307013].

[24] R. Narayanan, H. Neuberger and P. Vranas, *A simulation of the Schwinger model in the overlap formalism*, *Phys. Lett.* **B 353** (1995) 507 [hep-lat/9503013].

[25] H. Neuberger, *The overlap lattice Dirac operator and dynamical fermions*, *Phys. Rev.* **D 60** (1999) 065006 [hep-lat/9901003].

[26] C. Liu, *Hybrid monte carlo algorithm for lattice QCD with two flavors of dynamical Ginsparg-Wilson quarks*, *Nucl. Phys.* **B 554** (1999) 313 [hep-lat/9811008].

[27] A. Frommer, B. Nockel, S. Gusken, T. Lippert and K. Schilling, *Many masses on one stroke: economic computation of quark propagators*, *Int. J. Mod. Phys.* **C 6** (1995) 627 [hep-lat/9504020].

[28] A. Bode, U.M. Heller, R.G. Edwards and R. Narayanan, *First experiences with hmc for dynamical overlap fermions*, hep-lat/9912043.

[29] R. Narayanan and H. Neuberger, *An alternative to domain wall fermions*, *Phys. Rev.* **D 62** (2000) 074504 [hep-lat/0005004].

[30] A. Borici, A.D. Kennedy, B.J. Pendleton and U. Wenger, *The overlap operator as a continued fraction*, *Nucl. Phys.* **106** *(Proc. Suppl.)* (2002) 757 [hep-lat/0110070].

[31] L. Giusti, C. Hoelbling, M. Lüscher and H. Wittig, *Numerical techniques for lattice QCD in the epsilon-regime*, *Comput. Phys. Commun.* **153** (2003) 31 [hep-lat/0212012].

[32] P. Chen et al., *The finite temperature QCD phase transition with domain wall fermions*, *Phys. Rev.* **D 64** (2001) 014503 [hep-lat/0006010];
For recent proceedings contributions see L. Levkova and R. Mawhinney, *Improving dynamical domain-wall fermion simulations*, *Nucl. Phys.* **129** *(Proc. Suppl.)* (2004) 399 [hep-lat/0309122];
RBC collaboration, C. Dawson, *Dynamical domain wall fermions*, *Nucl. Phys.* **128** *(Proc. Suppl.)* (2004) 54 [hep-lat/0310055].

[33] J. van den Eshof, A. Frommer, T. Lippert, K. Schilling and H.A. van der Vorst, *Numerical methods for the QCD overlap operator, I. Sign-function and error bounds*, *Comput. Phys. Commun.* **146** (2002) 203 [hep-lat/0202025].

[34] T.-W. Chiu, T.-H. Hsieh, C.-H. Huang and T.-R. Huang, *A note on the Zolotarev optimal rational approximation for the overlap Dirac operator*, *Phys. Rev.* **D 66** (2002) 114502 [hep-lat/0206007].

[35] S. Duane, A.D. Kennedy, B.J. Pendleton and D. Roweth, *Hybrid Monte Carlo*, *Phys. Lett.* **B 195** (1987) 216.

[36] S.D. Katz, *Lattice QCD at finite T and μ*, *Nucl. Phys.* **129** *(Proc. Suppl.)* (2004) 60 [hep-lat/0310051].

[37] M. Golterman and Y. Shamir, *Localization in lattice QCD*, *Phys. Rev.* **D 68** (2003) 074501 [hep-lat/0306002].

[38] G. Arnold, N. Cundy, J. van den Eshof, A. Frommer, S. Krieg, T. Lippert and K. Schaefer, work in preparation.

JHEP08(2004)003